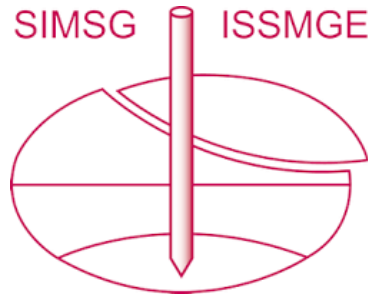


INTERNATIONAL SOCIETY FOR SOIL MECHANICS AND GEOTECHNICAL ENGINEERING



This paper was downloaded from the Online Library of the International Society for Soil Mechanics and Geotechnical Engineering (ISSMGE). The library is available here:

<https://www.issmge.org/publications/online-library>

This is an open-access database that archives thousands of papers published under the Auspices of the ISSMGE and maintained by the Innovation and Development Committee of ISSMGE.

The paper was published in the proceedings of the 10th European Conference on Numerical Methods in Geotechnical Engineering and was edited by Lidija Zdravkovic, Stavroula Kontoe, Aikaterini Tsiampousi and David Taborda. The conference was held from June 26th to June 28th 2023 at the Imperial College London, United Kingdom.

To see the complete list of papers in the proceedings visit the link below:

<https://issmge.org/files/NUMGE2023-Preface.pdf>

Investigating the impact of the climatic boundary conditions on the landslide reactivation of a clay slope: the Fontana Monte case study

A. di Lernia¹, G. Elia¹, F. Cotecchia¹

¹*Department of Civil, Environmental, Land, Building Engineering and Chemistry (DICATECh), Technical University of Bari, Bari, Italy*

ABSTRACT: The slope-vegetation-atmosphere (SLVA) interaction is considered the trigger of deep landslide activity in several clay slopes in the Italian Southern Apennines, where reactivations are associated to seasonal piezometric excursions connected to weather, influencing the water infiltration through the slope surface, as well as the hydraulic recharge of deep aquifers. The present paper reports an advancement in the SLVA interaction simulation of a prototype slope, the Fontana Monte slope (Vulturino, Italy), aimed at investigating the influence of the climatic hydraulic boundary conditions (HBCs) on both the piezometric fluctuations and the landslide reactivations. Transient uncoupled hydraulic (H) simulations associated to limit equilibrium (LE) analyses have been conducted by implementing the total rainfall time history occurring in the 2008-2020 monitored time as inflow flux and the evapotranspiration of two different plant types covering the slope surface as outflow flux. The H+LEM results show the extent to which the implementation of appropriate HBCs might provide accurate piezometric head fluctuations for a reliable prediction of the timing of landslide reactivations.

Keywords: Weather-induced landslides; Slope-Vegetation-Atmosphere interaction; Transient seepage analysis; Slope stability.

1 INTRODUCTION

The interaction of a vegetated ground surface with the atmosphere, referred to as “slope-vegetation-atmosphere (SLVA) interaction”, may affect the equilibrium conditions of a slope, location of either deep or shallow landslide mechanisms (Elia et al., 2017). Indeed, weather-related actions are deemed to play a great role on the landslide activity of clayey slopes location of deep landslides (Cascini et al. 2010). In the Italian south-eastern Apennines, most of the clay slope landslides suffers from weather-related reactivations connected to piezometric head fluctuations (Cotecchia et al., 2014; Losacco et al., 2021; di Lernia et al., 2022). Also, the hydrogeological set-up might govern the transient flow conditions in the slope, as in the case of slopes made of fine soils overlaying a rocky aquifer, representing a source of significant piezometric heads at depth. In such cases, the piezometric excursions might also be connected to the seasonal groundwater recharge of the deep aquifer. This scenario applies to the Fontana Monte hillslope, located in Vulturino (FG, southern Italy), selected as a prototype slope for the class of weather-induced landslides in the south-eastern sector of the Italian Apennines (Lollino et al., 2016; di Lernia et al., 2022, 2023). In this slope, the presence of a permeable rocky aquifer below a thick clay layer

causes high piezometric heads. The seasonal groundwater recharge of the deep aquifer is deemed to be responsible for the significant piezometric head fluctuations measured at large depths, while the fluctuations at shallower depths are mainly connected to the interaction of the topsoil with the atmosphere (di Lernia et al., 2022). In this work, the 2013-2014 thermo-pluviometric year, considered as an average climatic condition for the slope area, was implemented as inflow flux, while the evapotranspiration flux was evaluated assuming the winter wheat plant type, since the aim of the SLVA simulations was to identify the predisposing and triggering factors of the landsliding in the area.

In the present paper, the impact of different climatic hydraulic boundary conditions (HBCs) adopted at the top surface, such as the climatic year and the plant type, on both the piezometric fluctuations and the slope stability has been explored through transient seepage simulations, performed by means of an uncoupled hydraulic (H) finite element (FE) approach, associated to limit equilibrium (LE) analyses. Seepage analyses have been performed implementing the total rainfall time history occurring in the 2008-2020 monitored time as inflow flux at the slope ground surface, while two vegetation types have been considered to evaluate the evapotranspiration outflow flux.

2 THE FONTANA MONTE CASE STUDY

The Fontana Monte slope, representative of several clay slopes in the Italian south-eastern Apennines, is location of a large slow-moving deep-seated landslide, whose current activity has been found to be related to climatic actions, as the SLVA interaction processes affect both the hydrogeological boundary conditions at depth and at the outcropping ground surface (di Lernia et al., 2022, 2023). The landslide body, mainly involving the Toppo Capuana (TPC) clays, is about 1 km long and 300 m wide, with the toe at the Giardino stream (Figure 2a). The old town of Volturino lies on the limestone member of the Faeto Flysch (named FAEc herein), which is in contact, to the west, with the outcropping TPC clays and, to the east, with the outcropping clayey member of

the Faeto Flysch (named FAEa). Within the longitudinal Section 1 (Figure 2b), crossing the landslide body, the outcropping TPC formation overlies a sequence of FAEc, FAEa, Red Flysch (FYR) and Sub-Apennine Blue Clays (ASub) layers.

The current landslide activity is characterised by seasonal reactivations, with the rate of movements increasing in winter and reducing during the dry season (Figure 2c), as typically observed in other slopes in the same area. The piezometric head fluctuations, triggering the acceleration of the landslide body, are related to both the interaction of the ground slope with the atmosphere and the seasonal groundwater recharge of the deep aquifer, represented by the FAEc layer, as demonstrated through the transient seepage analyses discussed by di Lernia et al. (2022).

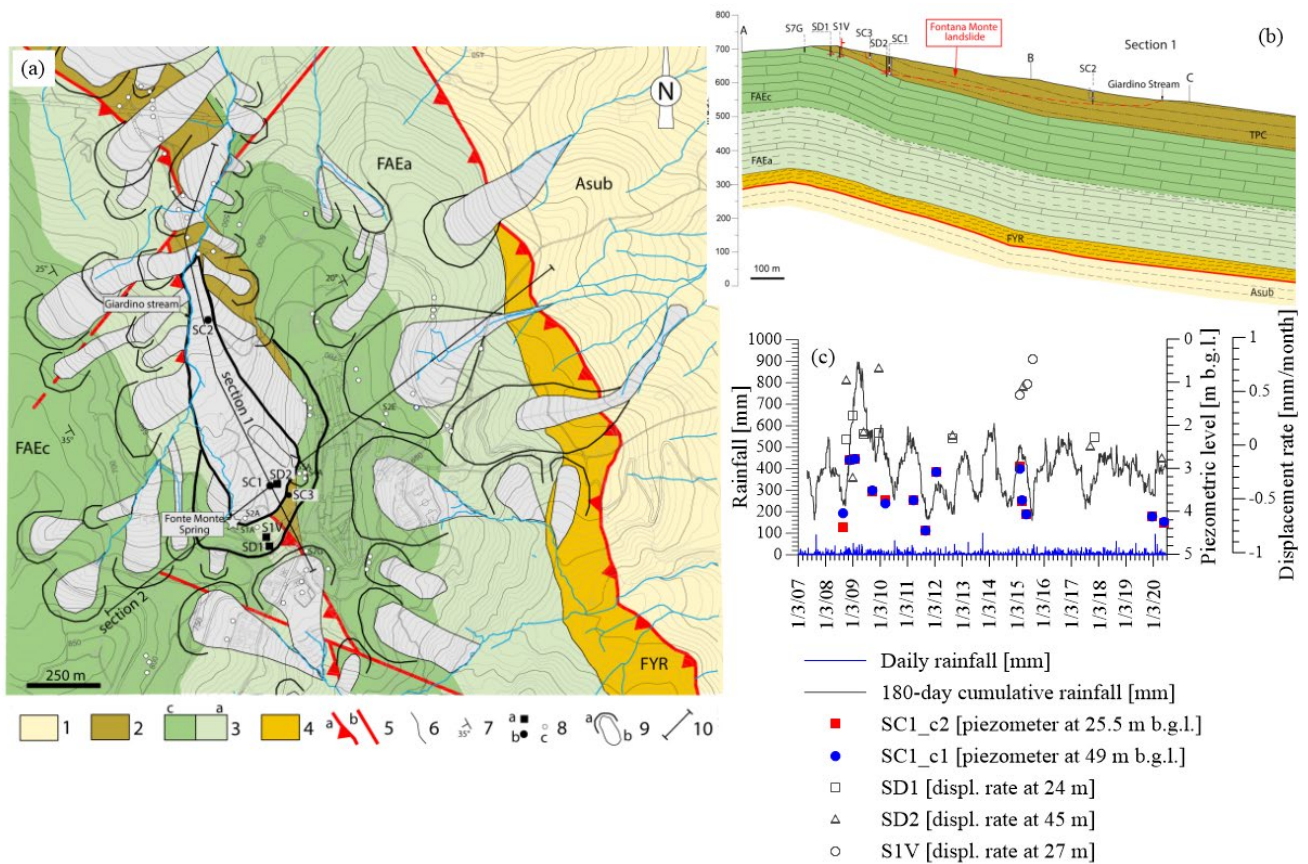


Figure 1. (a) Geological and geomorphological map; (b) longitudinal Section 1; (c) recorded rainfalls and in-situ monitoring data. Legend of Figure 1a: 1. ASub; 2. TPC; 3. Limestone member (FAEc) and clayey member (FAEa) of Faeto Flysch; 4. FYR; 5. Overthrust (a) and fault (b); 6. Stratigraphic contact; 7. Bedding (dip in degree); 8. Boreholes hosting inclinometer (a) or piezometer (b) drilled during the 2008-2012 campaigns; (c) previous field investigations; 9. Landslide (a-crown, b-body); 10. Cross section trace (modified after di Lernia et al. 2022, 2023)

3 MODELLING STRATEGY OF THE SLVA INTERACTION

The transient seepage across the Fontana Monte slope due to the SLVA interaction has been analysed through hydraulic uncoupled FE modelling, carried out using the software Seep/w (Geo-Slope International, 2004).

The resulting porewater pressure distribution has been, then, employed in LE analyses, conducted adopting the Morgenstern and Price method implemented in the software Slope/w (Geo-Slope International, 2004).

3.1 Numerical slope model

The analyses have been carried out with reference to the slope Section 1, crossing the landslide body along the

direction of maximum inclination (Figure 1). A mesh discretization with 6-noded triangular elements has been employed for the whole domain, while a more refined mesh, with elements of about 0.2 m, has been adopted close to the ground surface, where time dependent boundary conditions are applied during the transient seepage modelling (Figure 2). A 6 m thick layer of fractured clay (referred to as “fractured topsoil”), overlaying the TPC layer, has been implemented in the FE model. The hydraulic properties of the soil layers have been defined based on in-situ and laboratory tests, as described in Lollino et al. (2016) and di Lernia et al. (2022). The partially saturated response of the soils located above the water table has been simulated through the water retention curve (WRC), modelled according to van Genuchten (1980), and the hydraulic conductivity function, defined according to the Mualem’s formulation (Mualem, 1976), whose parameters have been calibrated based on literature data as described in di Lernia et al. (2022). The volumetric compressibility coefficient, m_v , has been assumed equal to $5 \cdot 10^{-5}$ 1/kPa for the fractured topsoil and 10^{-7} 1/kPa for the deeper soil layers. A summary of the hydraulic and retention parameters implemented in the H simulations is reported in Table 1.

Table 1. Hydraulic and retention parameters implemented in the hydraulic simulations.

Soil layer	θ_{sat} (%)	θ_{res} (%)	a (kPa)	n (-)	m (-)	k_{sat} (m/s)	m_v (1/kPa)
Fractured topsoil	45.5	5	135.7	1.21	0.171	10^{-8}	$5 \cdot 10^{-5}$
TPC	40	5	1694.9	2.33	0.572	10^{-9}	10^{-7}
FAEa	40	5	1694.9	2.33	0.572	$5 \cdot 10^{-8}$	10^{-7}
FAEc	35.7	2.5	3.8	1.69	0.408	$5 \cdot 10^{-6}$	10^{-7}

The summer-like steady-state HBC has been defined accounting for the three-dimensional hydrogeological set-up of the hillslope, as described in di Lernia et al. (2022) and illustrated in Figure 2. Free drainage has been imposed to the top boundary of the FE model to estimate the initial steady-state porewater pressure distribution, whose corresponding equipotential lines are shown in Figure 2. Then, transient seepage analyses have been carried out employing daily time steps of the climatic HBCs described in the next paragraph.

The predicted porewater pressure distribution, varying with time, has been employed in LE analyses, conducted using the Mohr-Coulomb failure criterion modified to account for the soil partial saturation above the water table according to the formulation proposed by Vanapalli et al. (1996):

$$\tau_f = c' + (\sigma_n - u_a) \tan(\varphi') + (u_a - u_w) \left[\left(\frac{\theta_w - \theta_r}{\theta_s - \theta_r} \right) \tan(\varphi') \right] \quad (1)$$

where θ_w is the current volumetric water content, θ_s and θ_r are the saturated and residual volumetric water content (for the TPC soil θ_r is equal to 12.5% of θ_s) and φ' is the mobilised friction angle, assumed equal to

19.2° as back-analysed by di Lernia et al. (2022) through LE along the pre-imposed slip surface indicated in Figure 2.

3.2 Evaluation of the climatic HBCs

The interaction between the slope, the vegetation and the atmosphere has been simulated through the application of climatic HBCs along the model boundaries. Since the hydraulic seepage in the Fontana Monte slope is also related to the seasonal recharge of the deep aquifer, the upstream HBC varies with time according to a sinusoidal law, oscillating between the summer-like and winter-like hydrostatic piezometric groundwater head, i.e. with water table between 3.5 m and 5 m b.g.l. (di Lernia et al., 2022). The HBCs applied to the ground surface have been evaluated as the difference between the inflow flux of the total daily rainfall and the outflow flux related to the daily evapotranspiration.

Following the approach proposed by Tagarelli and Cotecchia (2020), the total daily rainfall (Figure 3a) recorded at the Volturino weather station between 2008 and 2020 has been employed in the simulations. As typically observed in slopes in the same geo-hydro-mechanical context, the 180-day cumulative rainfall time history (shown in Figure 3a) is characterised by peaks always occurring in the late winter-early spring (between January and May). This pattern is clearly identifiable till the end of 2015, while a change in the weather conditions might be observed in the 2015-2020 period, during which the 180-day cumulative rainfall shows lower values distributed over a longer time period. Thus, in order to evaluate the actual interaction of the slope with the atmosphere, the total rainfall time history recorded in the entire monitoring time, i.e. 2008-2020, should be implemented in the simulations as inflow flux.

The daily evapotranspiration outflow fluxes have been estimated according to the “FAO Penman-Monteith method” through the dual crop coefficient approach (Allen et al., 1998). The crop evapotranspiration fluxes $ET_{c,adj}$ have been evaluated on a daily basis, splitting the evaporation flux, $E_{c,adj}$, and the transpiration flux, $T_{c,adj}$ through Eq. (2), valid for non-standard conditions:

$$ET_{c,adj} = E_{c,adj} + T_{c,adj} = (K_{e,adj} + K_{cb,adj}) ET_0 \quad (2)$$

$$K_{e,adj} = K_r (K_{c,max} - K_{cb,adj}) f_{ew} \quad (3)$$

$$\begin{cases} K_{cb,adj} = K_s K_{cb} f_c \\ K_{cb,adj} = (K_{cb} - A_{cm}) K_s \end{cases} \quad (4)$$

where ET_0 is the reference evapotranspiration, $K_{e,adj}$ is the adjusted soil evaporation coefficient (Eq. 3), which applies to the non-vegetated ground surface of the slope, and $K_{cb,adj}$ (Eq. 4) is the adjusted basal crop coefficient, depending on the type and growth of the vegetation during the year. K_{cb} is the basal crop coefficient in standard conditions, while $K_{c,max}$ is the maximum value of the crop coefficient, assumed equal to

$[0.05 + \max(K_{cb})]$. In Eq. 4, the first line is valid for the initial and late season growth stages, while the second one is used for the development and mid-season growth stages. K_r is the water stress coefficient, considering the effect of water stress on the crop transpiration. It has

been implemented in the numerical model as a function of the soil suction and calculated accounting for the maximum root depth of the plant and the volumetric water content at field capacity and at the wilting point with the procedure described by Allen et al. (1998).

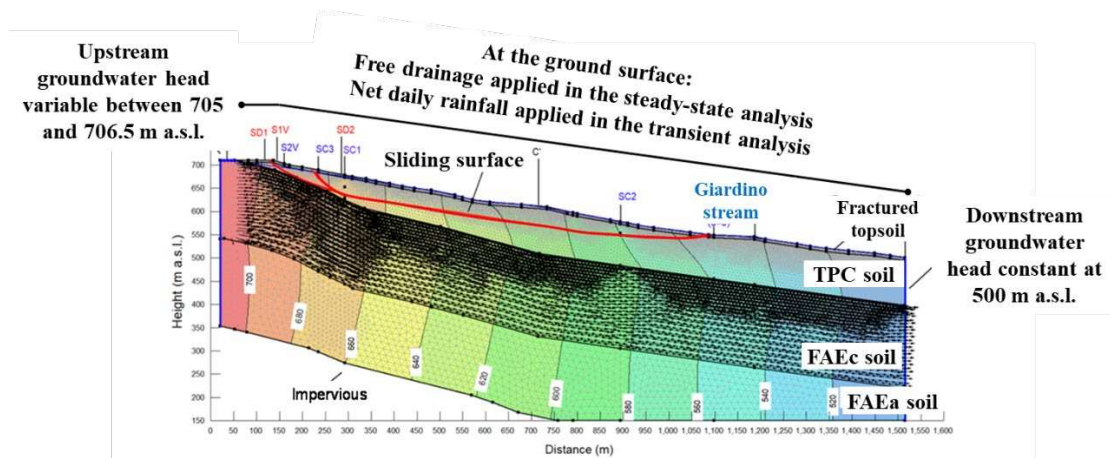


Figure 2. FE slope model, boundary conditions and equipotential lines obtained at the end of the steady-state seepage simulation

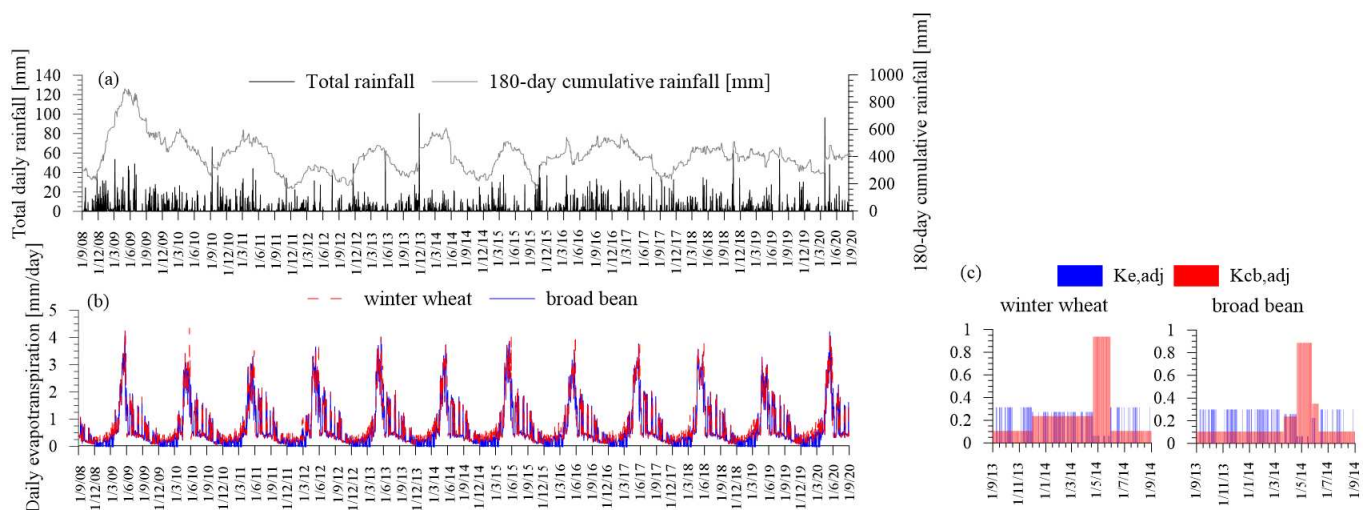


Figure 3. (a) Daily total rainfall and 180-day-cumulative rainfall and (b) daily evapotranspiration time history covering the period 1st September 2008-1st September 2020; (c) adjusted basal crop and evaporation coefficient curves for different types of vegetation

K_r is the soil evaporation reduction coefficient dependent on the cumulative depth of the water evaporated from the topsoil. It depends on the soil suction and its evaluation has been carried out considering the depth of the soil layer subjected to drying due to evaporation and the volumetric water content at both the field capacity and wilting point states (Allen et al., 1998). The coefficient f_{ew} , equal to $[\min(1-f_c; f_w)]$, is the portion of the soil surface exposed to evaporation, where f_c is the average fraction of soil surface covered by vegetation and f_w is the portion of the soil surface wetted by precipitation (equal to 1 for rainy days and 0 for dry days). A_{cm} is the adjustment coefficient for sparse vegetation (Allen et al., 1998).

In the present study, two types of vegetations, observed to be cultivated in-situ, i.e. the winter wheat and the broad bean, have been assumed to cover on average the 70% of the slope surface constantly throughout the year. The basal crop coefficient values K_{cb} assumed for each growth period and different plant types are summarised in **Error! Reference source not found.** The adjusted basal crop coefficient and evaporation coefficient curves are illustrated Figure 3c. The different duration of the crop growth stages for the two types of vegetation implies different amounts of the evaporation and transpiration components. The resulting daily evapotranspiration fluxes are characterised by similar shapes, with a higher extraction of water during winter (i.e. Dec – Mar) for the winter wheat (Figure 3b).

Table 2. Basal crop coefficients and fraction of soil surface covered different types of vegetation.

Vegetation type	Winter wheat				Broad bean			
Growth stage	Initial	Crop development	Mid-season	Late	Initial	Crop development	Mid-season	Late
Period of the year	1/11-30/11	1/12-19/04	20/04-29/05	30/05-28/06	1/03-20/03	21/03-19/04	20/04-24/05	25/05-8/06
Duration	30 days	140 days	40 days	30 days	20 days	30 days	35 days	15 days
K_{cb}	0.15	0.4	1.05	0.15	0.15	0.4	1.05	0.5

According to the simple root-water uptake model, the evaporation flux has been implemented at the depth of 0.05 m, the transpiration flux has been applied at one-third of a root depth of 0.75 m, i.e. 0.25m b.g.l., while the total rainfall has been prescribed at the top ground surface. The runoff has been computed by imposing that the porewater pressure becomes zero at the ground surface when the piezometric head equals the geometric head.

4 IMPACT OF CLIMATE ON PIEZOMETRIC REGIME AND SLOPE STABILITY

The results of the transient seepage analyses are illustrated in terms of variation with time of the piezometric heads predicted at 25.5 m (SC1_c2) and 49 m (SC1_c1) b.g.l. along the SC1 vertical, and compared to in-situ measured data (Figure 4). The numerical results obtained by di Lernia et al. (2022), adopting the 2013-2014 year cycled 12 times and assuming the slope surface covered by winter wheat, are also shown for reference in the same figure. In general, the response at 49 m depth is slightly affected by the top HBC. Conversely, the climatic top boundary significantly influences the piezometric head fluctuations at the lower monitored depth, i.e. 25.5 m b.g.l. In the case of winter wheat covering the slope surface, the simulation implementing the 2008-2020 climatic boundary provides a more realistic estimation of the piezometric level oscillations with respect to the one obtained considering the 2013-2014 representative year, since the timing and the values of the piezometric head peaks are more coherent with both the in-situ piezometric data and the 180-day cumulative total rainfall. When the broad bean is considered, due to the shorter duration of the crop development and mid-season growth stages, the piezometric head peaks are greater than those exhibited by the winter wheat plant type. Indeed, the duration of the growth stages strongly affects both the evaporation and the transpiration component of the outflow fluxes, generating a higher amount of water infiltrating in the slope, which in turn affects the piezometric level fluctuations.

The impact of the climatic boundary on the stability of the slope has been estimated, then, by computing the variation of the factor of safety (FS) of the landslide body for the pre-imposed slip surface shown in Figure 2. The time variation of the normalized FS/FS_{init} , where FS_{init} is the factor of safety evaluated at the end of the

summer-like steady-state hydraulic simulation, is reported in Figure 4, together with the few available inclinometric data at the shear band depth along the SD1 and SD2 verticals, shown in terms of displacement rates, to identify the timing of landslide reactivations.

It might be observed that the top HBCs strongly affect the time variation of FS of the slip surface, although its location is at a depth of about 50 m b.g.l. Moreover, the different climatic years occurring between 2008 and 2020 cause some differences in the time variation of the normalised factor of safety with respect to the representative 2013-2014 climatic year, in terms of both timing and peak values. Indeed, while the instability condition (i.e. $FS/FS_{init}=1$) is regularly achieved always during winter (i.e. Dec – Mar) for the representative year (red line), the landslide reactivations predicted by the 2008-2020 simulations are observed once the piezometric head reaches significant peak values. This trend is recognisable by the in-situ inclinometric monitoring data (Figure 4), showing displacement rates greater than zero (full dots) just before the minimum values of the FS/FS_{init} curves and about zero (empty dots) whenever the FS/FS_{init} curves achieve the maximum values. Also, the two plant types generate different patterns of the normalised FS of the landslide body, which oscillates between minimum and maximum values of different intensities depending on the piezometric head fluctuations. Indeed, due to the lower evapotranspiration capacity of the broad bean, causing higher piezometric heads at shallow depths, the instability threshold is reached more frequently than in the case of the winter wheat, implying landslides reactivations which have not been recorded by the instruments, as for example in Dec 2010 – Mar 2011, Dec 2013 – Mar 2014, Jan 2018 – May 2018. Nevertheless, it should be remarked that additional and more frequently recorded in-situ data would finalise the validity of the numerical approach for predictive purposes.

5 CONCLUSIONS

The paper presents an advancement in the SLVA interaction simulation of the Fontana Monte prototype slope, representative of deep-seated and slow weather-related landsliding. The transient H+LEM analyses allowed to quantify the influence of the climatic hydraulic boundary conditions applied at the top surface on both the hydraulic response of the slope and its stability. The results suggested that the use of the climatic year covering the entire monitoring time 2008-2020 is necessary

to accurately evaluate the timing of landslide reactivations. Moreover, the cultivation of specific plant types, like the broad bean, might increase the instability conditions of the slope. In conclusion, the H+LEM numerical modelling can be considered a reliable tool for the

prediction of landslide reactivations, providing that appropriate climatic boundary conditions are selected as input of the simulations.

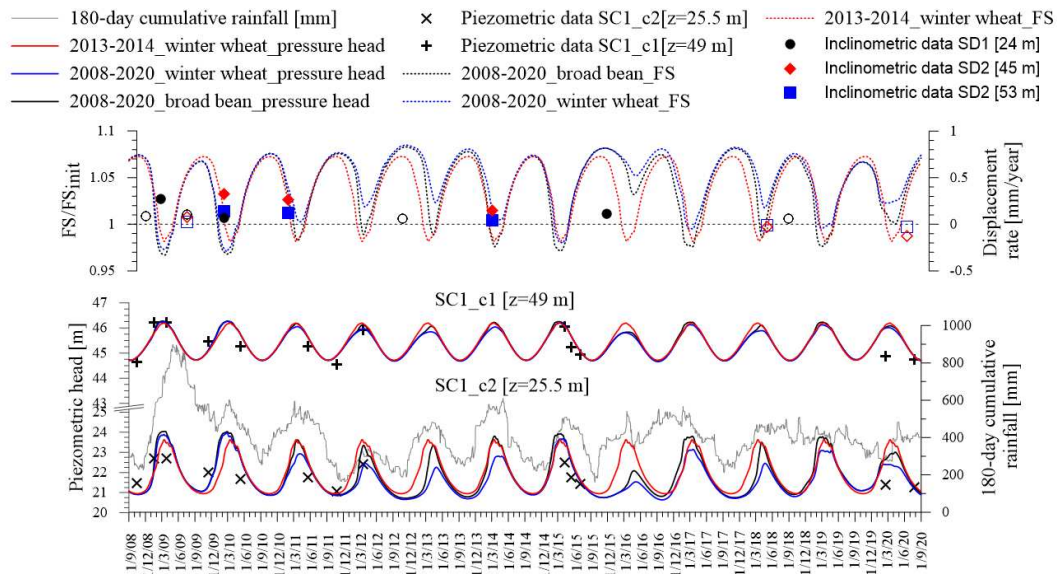


Figure 4. Comparison of the monitored and predicted piezometric heads at 25.5 m (SC1_c2) and 49 m (SC1_c1) and variation with time of the normalised FS of the landslide body (dashed lines) compared to the inclinometric data (full dots correspond to reactivations periods, empty dots represent period without movements).

6 ACKNOWLEDGEMENTS

The research has been supported by the PON-AIM project (AIM1871082) and the PON-MITIGO project (ARS01_00964). Since 1st September 2022, F. Cotecchia and G. Elia contributed through the project “National Centre for HPC, Big Data and Quantum Computing – Spoke 5: Environment and Natural Disasters” (CN_00000013) funded by the National Recovery and Resilience Plan (NRRP).

7 REFERENCES

- Allen, R.G., Pereira, L.S., Raes, D., Smith, M. 1998. Crop evapo-transpiration (guidelines for computing crop water requirements), in: FAO Irrigation and Drainage Paper No. 56. Rome, Italy.
- Cascini, L., Cuomo, S., Pastor, M., Sorbino, G. 2010. Modeling of Rainfall-Induced Shallow Landslides of the Flow-Type. *J. Geotech. Geoenvironmental Eng.* **136**, 85–98.
- Cotecchia, F., Pedone, G., et al. 2014. Slope-atmosphere interaction in a tectonized clayey slope: a case study. *Ital. Geotech. J.* **1**, 34–61.
- di Lernia, A., Cotecchia, F., Elia, G., et al. 2022. Assessing the influence of the hydraulic boundary conditions on clay slope stability: The Fontana Monte case study. *Eng. Geol.* **297**.
- di Lernia, A., Cotecchia, F., Elia, G., Tagarelli, V., Santaloia, F., Palladino, G. 2023. Combined use of hydraulic and coupled hydro-mechanical numerical modelling of the response of a clay slope to climatic actions in the long term. *Ital. Geotech. J.*, accepted.
- Elia, G., Cotecchia, F., Pedone, G., Vaunat, J., et al. 2017. Numerical modelling of slope-vegetation-atmosphere interaction: an overview. *Q. J. Eng. Geol. Hydrogeol.* **50**, 249–270.
- Geo-Slope International. 2004. GeoStudio, User’s guide.
- Lollino, P., Cotecchia, F., Elia, G., Mitaritonna, G., Santaloia, F. 2016. Interpretation of landslide mechanisms based on numerical modelling: two case-histories. *Eur. J. Environ. Civ. Eng.* **20**, 1032–1053.
- Losacco, N., Bottiglieri, O., Santaloia, F., Vitone, C., Cotecchia, F. 2021. The Geo-Hydro-Mechanical Properties of a Turbiditic Formation as Internal Factors of Slope Failure Processes. *Geosciences* **11**, 429.
- Mualem, Y. 1976. A new model for predicting the hydraulic conductivity of unsaturated porous media. *Water Resour. Res.* **12**, 513–522.
- Tagarelli, V., Cotecchia, F. 2020. Deep Movements in Clayey Slopes Relating to Climate: Modeling for Early Warning System Design, in: *Lecture Notes in Civil Engineering*. Springer, pp. 205–214.
- van Genuchten, M.T. 1980. A Closed-form Equation for Predicting the Hydraulic Conductivity of Unsaturated Soils. *J. Soil Sci. Soc. Am.* **44**, 892–898.
- Vanapalli, S.K., Fredlund, D.G., Pufahl, D.E., Clifton A W. 1996. Model for the prediction of shear strength with respect to soil suction. *Can. Geotech. J.* **33**, 379–392.